Eur. Phys. J. C (2025) 85:1470
https://doi.org/10.1140/epjc/s10052-025-15231-5

THE EUROPEAN PHYSICAL JOURNAL C

Check for updates

Regular Article - Theoretical Physics

$GW230529$: unveiling the hidden realm of the anisotropic neutron stars in the lower mass gap with gravitational wave echoes

Mayukh Bandyopadhyay[a]

Department of Physics, Jadavpur University, Kolkata, West Bengal 700032, India

Received: 8 November 2025 / Accepted: 13 December 2025

Abstract Recent discovery of a compact binary coalescence through $GW230529$ by LIGO has indicated the merger event of a compact object of mass between $2.5-4.5\ M_\odot$ with a neutron star of mass between $1.2-2.0\ M_\odot$. The mass of the unknown compact object makes it within the heaviest neutron star never tracked out or the lightest black hole ever detected. Here, we have shown that such a mass gap neutron star with this observed mass ($2.5-4.5\ M_\odot$) can be explained consistently by $f(R)$ gravity. We have also adopted the presence of pressure anisotropy inside the neutron star which supports a massive neutron star with mass more than $2.6\ M_\odot$, compatible with LIGO data ($GW190814$). Further, the modified Tollman–Oppenheimer–Volkoff equations have acknowledged such a compact stellar structure that can produce gravitational wave echoes (frequencies remain in the range of $3-6$ kHz).

1 Introduction

Till now, it is very well understood that the general relativity (GR hereafter) theory can relate the spacetime geometry based on the presence of the amount of matter and energy within it. We can apply GR successfully to explain the behavior of various compact objects in the strong field regime and also for the objects in the solar system [1–3]. Moreover, various observations through Event Horizon telescope have also confirmed its predictions as well [4,5]. But, still GR has faced some difficulties to solve the mysteries related to dark matter (DM hereafter) and dark energy (DE hereafter). The observational evidence of the present accelerating phase of the universe can not be well explained by using GR [6–10]. Furthermore, this theory is not able to give a singularity free stable structure of the relativistic compact objects like Neutron Stars (NSs hereafter). Under these circumstances, scientists suggest that the modification of GR should be required in order to solve these puzzles [11]. Beside, the much awaited quantum theory of gravity which can be constructed from the modifications of GR under the quantum corrections are widely accepted. Again, in case of low energy scale, the Einstein–Hilbert action of GR can be treated as a classical approximation also. In case of the Riemannian formulation of GR, gravitational effects can be recovered from the curvature of the spacetime manifold itself.

Nowadays, researchers are very interested in alternative theories of gravity with higher order nonlinear terms of curvature [12–16]. Amongst various modified gravity theories [17–23], $f(R)$ gravity theory is very simple, easily understandable and possesses some unique features also [24–28]. The $f(R)$ gravity generalizes the Ricci scalar R in the field equations of GR, which can explain cosmic acceleration easily. Further, this theory offers a very promising alternative way to explain the accelerated expansion of the universe by incorporating alternative ideas of DM and DE. The $f(R)$ also serves as the theoretical way out to examine gravity in the astrophysical and cosmological scales. In particular, in the case of $f(R)$ gravity, the matter Lagrangian can be considered as a generic function of the Ricci curvature scalar. Furthermore, for $f(R) \to R$, the theory of standard GR can be retraced and the standard Tolman–Oppenheimer–Volkoff (TOV hereafter) equations can be recovered. Through the past years several pioneering works on the compact objects have been done where the importance and significance of $f(R)$ gravity has been explored successfully [29–33]. These studies clearly depict the crucial impact and significance of the $f(R)$ gravity to investigate the astrophysical compact objects like NSs and black holes (BHs hereafter) under the present accelerating universe.

The presence of anisotropic matter distribution inside the stars (with pressure difference in the radial and trans-

[a] e-mail: mayukhbandyopadhyay@yahoo.com (corresponding author)

verse direction) is very significant, especially studying the astrophysical massive compact objects like NSs and BHs. The anisotropic matter distribution actually offers a way to examine the nature of matter under extreme environments (extreme gravitational conditions with tremendous high density and temperature). The models of the NSs with pressure anisotropy lead to very effective and accurate models of their stable internal structure. Further, this type of models also provide deeper understanding on the hydrostatic equilibrium of the stars and the maximum mass they can possess before their collapse [13,18,23,34–36]. On the other hand, in case of BH studies the anisotropic matter distribution also can influence the singularities and gravitational collapse dynamics [37,38]. At the same time, the presence of anisotropic matter significantly affects the cosmic structure formation and also the evolution of the universe [39–41]. In recent times, various significant models in modified gravity theories especially in $f(R)$ gravity considering the anisotropic matter distribution have successfully investigated the structural evolution and physical properties of the massive compact objects [42–46].

Moreover, the idea of incorporating the pressure anisotropy to investigate various crucial properties of the massive NSs, is not only reasonable for its prospective existence in case of highly dense matter present at the core of these compact objects but also by its essential appearance during the dynamical evolution of such kind of self-gravitating systems. In the pioneering work by Herrera [105], it is shown very elegantly that the physical processes which are naturally involved in case of the stellar evolution, particularly the dissipative mechanisms tend to produce significant pressure anisotropy even when the initial system configuration is under strictly isotropic considerations. Most importantly, it is also notable that at the final stage of such a dynamical evolution process in case of these massive compact stars, the initially generated pressure anisotropy will not disappear, rather its significant presence plays a very crucial role to maintain the final equilibrium configuration of the total system. Consequently, it is very interesting for the researchers to investigate compact objects with initially isotropic pressure but also exhibit anisotropic stresses in their final equilibrium configuration. This commencing insight certainly provides a very strong physical justification for adopting anisotropic fluid models of the massive NSs. Furthermore, this also significantly reinforces to come back from the pressure-isotropy assumption in the case of realistic stellar modeling.

Till now, many researchers have successfully applied the polytropic equation of state (EoS hereafter) to model and investigate the crucial properties of the relativistic compact objects [47–51]. More precisely, the polytropic EoS play a very significant role to study the internal structure of the compact objects and this type of EoS has a very crucial impact on the successful modeling and investigating the structural evolution of the astrophysical compact objects [52–56]. Moreover, the models of anisotropic compact stars in $f(R)$ gravity with the polytropic EoS has also become very popular amongst the researchers as these models have provided a deeper insight for the massive compact stars [57–61].

The NSs can be traced by GR in the strong field scenario but it gives a strict mass limit of those compact astrophysical objects which is about $1.44M_{\odot}$ and famous as Chandrasekhar's mass limit [62]. These objects have a stable configuration with radius about 10 km. Unfortunately, GR is not able to explain a more massive but stable compact structure beyond this mass limit [63–66]. But, some recent observations through GWs have found that some NSs can disobey this limit and scientists have predicted the existence of massive NSs in the lower mass gap (the mass is in between the heaviest NS and the lightest BH) [67–69]. Recently the GW observation $GW230529$ by LIGO (binary merger event of a NS and a mass gap (MG hereafter) compact object), have detected a compact object with mass about $3.66^{+0.82}_{-1.21}$ (in the mass range between $2.5-4.5\ M_{\odot}$) which clearly lies in the lower mass gap [70]. Further, from the observational point of view, accurate determination of mass of these types of compact objects can be achieved only for the NSs in the binary system [71,72]. Scientists are very enthusiastic that it might be the most massive NS ever observed. The NSs which give the opportunity to test gravity in a strong field regime, their internal structure can not be easily understood under extreme conditions. The way out to understand those supermassive compact objects is to apply modified theories of GR and to find some exotic but realistic EoS which can provide the stable massive compact configuration. In principle, with the given EoS, the mass–radius relation and the corresponding maximal mass can be obtained and also we can get the crucial information on the mechanism of its stability and possible impacts on the evolution of the NSs. In particular, the $f(R)$ gravity has also been successfully implemented to get the theoretical solution and to solve a lot of astrophysical issues [73–80].

The study of these types of supermassive and ultra-dense compact objects from the GWs observations lead to realize the internal matter configuration and also give deeper understanding on the structural and physical evolution of those relativistic compact objects under the present accelerating universe. Significantly, due to the ultra-dense compact structure, these objects can also produce the echo of the infalling GWs on their surfaces [81–84]. The possibility of the production of the gravitational wave echoes (GWEs hereafter) from the ultra dense compact objects were first introduced in the work [85]. In particular, these massive and highly dense compact objects should have the photon sphere outside their stellar structure to reflect the infalling GWs on them which actually creates the echoes. In some research, the frequency of the GWEs has been reported as in the range of kHz [86–90]. The production of the GWEs from the compact stars in

$f(R)$ gravity has also been investigated in the reference [91]. So, the GWEs can also be treated as the testing tool for the different compact star models in modified gravity theories also.

Following the above research and spirit, in the context of astrophysical observation $GW230529$, in this work the primary objective is to obtain the mass–radius relationship of the supermassive NSs and to derive the maximum mass limit which can be possessed by a NS under stable configuration with the realistic EoS. We also want to demonstrate that in the framework of modified gravity theories, the existence of supermassive NSs can also be explained successfully. At the same time, the GWEs also strongly support their existence. Significantly, in case of the Model-I, we have incorporated a general EoS to study the properties of the mass gap (MG) compact object but in case of the Model-II, we have chosen KB ansatz instead of a EoS for our investigation. These two unique models in the framework of $f(R)$ modified gravity have been tested rigorously which have significantly reshaped our conventional understandings on the supermassive NSs in the lower mass gap domain. Moreover, the obtained $mass-radius$ curves through modified TOV equations according to the model parameters with valid physical range can help to constrain various observable properties of the massive NSs as well. Further, the crucial impact of the pressure anisotropy on the supermassive stable structure of the NSs with hydrostatic equilibrium under spherical symmetry has been investigated very carefully.

This paper is organised as follows. In Sect. 2, we will briefly summarize the basic equations of the modified $f(R)$ gravity mathematically. In the next section, we will propose our present model and determine the model parameters, using matching conditions and applying proper boundary conditions. Section 4, will give full physical analysis of this present work with detailed explanation of physical quantities measured during this investigation. Here, we will also demonstrate the physical viability of this current model by using graphical variations of different parameters. Finally, in Sect. 5, we will briefly discuss and conclude the entire work. Throughout the investigation we have considered the unit $c = 8\pi G = 1$.

2 Stellar structure in $f(R)$ gravity: basic mathematical formulation

In this section we have discussed elaborately the derivation of the basic stellar equations in the framework of modified $f(R)$ gravity. The field equations are also obtained after solving the basic stellar equations.

Here, we have introduced the Einstein–Hilbert action in $f(R)$ gravity theory as

$$S_{f(R)} = \frac{1}{2}\int d^4x\sqrt{-g}[f(R) + \mathbf{L_M}], \tag{1}$$

where g denotes the determinant of the metric tensor g_{ab} and the matter Lagrangian is denoted by $\mathbf{L_M}$. Now, after applying the variation on g_{ab} in the Eq. (1), we have obtained the field equation for $f(R)$ as

$$\frac{df(R)}{dR}R_{ab} - \frac{f(R)}{2}g_{ab} + \left[g_{ab}\Box - \nabla_a\nabla_b\right]\frac{df(R)}{dR} = T_{ab}, \tag{2}$$

where T_{ab} denotes the energy momentum tensor, ∇_a represents the covariant derivative operator and $\Box \equiv \nabla_a\nabla^a$. The energy-momentum tensor for the anisotropic perfect fluid can be represented as

$$T_{ab} = \left[(p_t + \rho)\, U_a U_b - p_t g_{ab} + (p_r - p_t)V_a V_b\right], \tag{3}$$

where ρ, p_r and p_t denote the energy density, radial pressure and tangential pressure of the core fluid matter inside the NSs respectively. Further, U_a and V_a denotes the four-velocity and space-like four vectors of the fluid respectively and satisfy the normalization properties as $U_aU^a = 1$, $V_aV^a = -1$ and $U^aV_a = 0$. Now, the Eq. (2) can be represented as

$$G_{ab} = \frac{1}{f_R}\left[\tilde{T}_{ab} + T_{ab}\right] \equiv \tilde{T}_{ab}, \tag{4}$$

where G_{ab} denotes the Einstein tensor, $f_R \equiv \frac{df(R)}{dR}$ and the modifications from the higher order nonlinear terms of $f(R)$ is absorbed in $\tilde{T}_{ab}$. The effective stress-energy tensor $\tilde{T}_{ab}$ of $f(R)$ fluid is given by

$$\tilde{T}_{ab} = \left[\nabla_a\nabla_b f_R - \Box f_R g_{ab} + \{f - Rf_R\}\frac{g_{ab}}{2}\right]. \tag{5}$$

We have adopted the metric signature $(+,-,-,-)$. We have assumed the static metric for the spherically symmetric system has the form as

$$ds^2 = e^{A(r)}dt^2 - e^{B(r)}dr^2 - r^2d\theta^2 - r^2\sin^2\theta d\phi^2,$$
$$0 \le \theta \le \pi,\;\; 0 \le \phi \le 2\pi, \tag{6}$$

where $A(r)$ and $B(r)$ depends only on the radial coordinate r. Again, the energy-momentum tensor T_{ab} in the diagonal form can be written as

$$\tilde{T}_{ab} = diag\left(e^{\frac{A(r)}{2}}\rho, e^{\frac{B(r)}{2}}p_r, r^2p_t, r^2p_t\sin^2\theta\right). \tag{7}$$

3 Proposed stellar models in $f(R)$ gravity

In this section we have considered two different types of physically valid and suitable functional forms of $f(R)$ functions and also derived the modified TOV equations for both the cases. It is our main aim to explain the existence of supermassive NSs consistently assuming minimal modifications to GR. We have also incorporated the Buchdahl metric-I [92] and realistic EoS for our work. Significantly, our description can explain massive NSs which is more massive than what we have got from standard GR with stiffer EoS [66].

3.1 Model-I

The Buchdahl metric-I is given as

$$e^{B(r)} = \frac{L\left(1+\tau r^2\right)}{L-\tau r^2}, \tag{8}$$

where L and τ are constants. Significantly, the value of L depicts the regularity of the metric potentials at the centre of the star and higher values of τ ensures the more compact configuration. Here we have considered $f(R)$ as [93]

$$f(R) = R + \xi R^2, \tag{9}$$

where ξ is the coupling parameter. In particular, this model is very suitable to explain the accelerated expansion of the universe with higher order curvature terms [94]. The associated Ricci scalar can be written as

$$R(r) = \frac{e^{-B(r)}}{2r^2}\Big[4rA(r)' + r^2A(r)'^2 + 2r^2A(r)'' - r^2A(r)'B(r)' - 4rB(r)' - 4e^{B(r)} + 4\Big]. \tag{10}$$

Now, solving the Eqs. (4), (6) and (7), we have obtained the field equations as

$$\rho = \frac{e^{-B(r)}}{2r^2}\Big[Rr^2e^{B(r)}f_R + r^2B(r)'f_R' + 2f_R - 2f_Re^{B(r)} - 2r^2f_R'' - 2rB'(r)f_R - 4rf_R' - r^2fe^{B(r)}\Big], \tag{11}$$

$$p_r = \frac{e^{-B(r)}}{2r^2}\Big[r^2e^{B(r)}f + 2e^{B(r)}f_R + 2rf_RA'(r) + 4rf_R' + r^2A'(r)f_R' - 2f_R - r^2Re^{B(r)}f_R\Big] \quad and \tag{12}$$

$$p_t = \frac{e^{-B(r)}}{2r^2}\Big[2f_RB'(r) + 4f_R' + 2rA'(r)f_R' + 4rf_R'' + 2rfe^{B(r)}\Big] + \frac{e^{-B(r)}}{2r^2}\Big[-2rf_RA''(r) - rf_RA'^2(r) - rA'(r)B'(r)f_R - 2A'(R)f_R - 2rB'(r)f_R'' - 2rRf_Re^{B(r)}\Big]. \tag{13}$$

Further, we have also incorporated the polytropic EoS as

$$p_r = H\rho + K\rho^{(1+\frac{1}{n})}, \tag{14}$$

where H and K are the proportionality constants, n denotes the polytropic index. The parameter H actually indicates the stiffness of the EoS and higher values of H signifies the more stability of the compact object with stiffer EoS. On the other hand, the parameter K actually controls the repulsive effects inside the star which also confirms the stability of the star by opposing the collapse under extreme inward gravitational force. The polytropic index n which is also known as the nonlinearity index, mainly affects the compactness of the star and its value lies in the range $0 < n < 1$.

Now, using the filed Eqs. (11) to (13) and employing the Eqs. (8), (9), (10) and (14), we have got the expressions of energy density ρ, radial pressure p_r and p_t as

$$\rho = 5.36521457\times10^6 \times \frac{(1+L)\tau^2}{L^3(1+\tau r^2)}\Big[\Big\{-46\xi\tau^2 + 26r^6\tau^3 + L^2(54+39r^2-72\xi)\tau + 38r^6\tau^2\xi^2\Big\}\Big], \tag{15}$$

$$p_r = 3.2874526\times10^{15} \times\frac{\tau(1+L)}{L^6(1+\tau r^2)}\Big[HL^3(1+\tau r^2)^9\Big] \quad and \tag{16}$$

$$p_t = 2.65378942\times10^{18}\times\frac{\tau(1+L)}{L^3(L-\tau r^2)^2(1+\tau r^2)^{10}}. \tag{17}$$

The anisotropic factor can be measured as

$$\Delta = p_t - p_r \quad (p_t > p_r). \tag{18}$$

Interestingly, the radial pressure p_r varies differently from the transverse pressure p_t. Due to this difference in pressure inside the NSs, anisotropic force comes into play inside. The anisotropic force(Δ')in $f(R)$ modified gravity can be obtained as

$$\Delta' = \frac{2}{r}\Delta. \tag{19}$$

This model gives $\Delta' > 0$ which means $p_t > p_r$ for the NSs under the study.

We have matched the interior spacetime metric to the exterior spacetime metric at the boundary surface $r = \mathbf{R}$ of the star to make the Ricci scalar and its normal derivative continuous at the boundary surface with the metric potentials in $f(R)$ gravity [95]. The external metric can be written as

$$ds^2 = -\left(1-\frac{2M}{r}\right)dt^2 + \frac{dr^2}{(1-\frac{2M}{r})} + r^2(\sin^2\theta d\phi^2 + d\theta^2), \tag{20}$$

where M represents the total mass of the star within the boundary ($r = \mathbf{R}$). Moreover, at the boundary surface, the spacetime variables like g_{tt}, g_{rr} and $g_{tt,r}$ are continuous between the exterior and interior metrics i.e. $g_{rr}^- = g_{rr}^+$ *and* $g_{tt}^- = g_{tt}^+$ and yield the following relations as

$$\left(1-\frac{2M}{\mathbf{R}}\right)=e^{A(r)}=e^{-B(r)} \quad and \tag{21}$$

$$p_r(r=\mathbf{R})=0. \tag{22}$$

Now, from the smooth matching across the boundary surface and using the Eqs. (15) to (17), (21) and (22), we have obtained the required model parameters as

$$\tau=\frac{2Lu(r)}{r^2\{1+L-2Lu(r)\}} \quad and \tag{23}$$

$$K=3.6584687512\times HL^3(1+\tau r^2)^9, \tag{24}$$

where $u(r)$ is the compactness factor of the concerned mass gap compact object under investigation.

Now, using the above Eqs. (23) and (24) along with the expression of ρ we have obtained the central pressure (p_c), surface energy density (ρ_s) and central energy density ρ_c as

$$p_c=5.283146\times 10^{18}\times\tau\frac{(1+L)}{L^6}\Big[H\{38L^3\tau^2\xi-42L\xi^2\tau-K\tau(1+L)\xi-56L^2\tau^2\}\Big], \tag{25}$$

$$\rho_s=4.243871\times 10^4\times\tau\frac{(1+L)}{L^3}\Big[\{35\xi\tau^2-L^2 28\tau\xi-2L\tau(24+36\xi)\}\Big] \quad and \tag{26}$$

$$\rho_c=4.657234\times 10^6\times\tau\frac{(1+L)}{L^3}\Big[28\xi\tau\{(56+24L^2)+54L\tau-16\tau\}\Big]. \tag{27}$$

3.2 Model-II

In this new model, we also want to check that another completely different framework of $f(R)$ gravity is able to explain the existence of the supermassive NSs in the lower mass gap or not. In this approach we have considered the $Krori-Barua$ (KB hereafter) ansatz which has been employed as an alternative to the EoS. The KB ansatz effectively establishes the relations between the pressures and density of the compact object as well. Now, we have considered another interesting model where $f(R)$ is chosen as

$$f(R)=Re^{\kappa R}=R+\kappa R^2+\frac{1}{2}\kappa^2R^3+........, \tag{28}$$

where κ is denoted as a dimensional quantity in squared length units. For $\kappa=0$, the standard GR can also be recovered. Interestingly, in this framework the negative values of κ also provide the massive NSs with maximum compactness and also satisfy the Buchdahl limit. Surprisingly, this clearly contrasts with GR or even other $f(R)$ gravity theories with positive κ. This model can also predict the existence of supermassive NSs in the lower mass gap with very high central density (much higher compared to the nuclear saturation density $\rho_{nuc}=3\times 10^{14}\ g\ cm^{-3}$). Moreover, we have also obtained the mass–radius relationship which is very much consistent with other observational data. The metric potentials as in Eq. (6) in terms of the KB ansatz can be written as

$$A(r)=s_0\left(\frac{r}{\mathbf{R}}\right)^2+s_1 \quad and \tag{29}$$

$$B(r)=s_2\left(\frac{r}{\mathbf{R}}\right)^2, \tag{30}$$

where s_0, s_1 and s_2 are the dimensionless parameters and can be determined from the boundary conditions with the help of the exterior metric as given in Eq. (20).

Now, in this case the associated scalar curvature equation can be written as

$$3e^{-B(r)}\left[\left\{\frac{1}{r}+A^{'}(r)-B^{'}(r)\right\}f_R^{'}+f^{''}(R)\right]=(p_r+2p_t-\rho)+2f-Rf_R. \tag{31}$$

The field equations can be written as

$$8\pi\rho=\frac{f_R}{r^2}\left\{1-\frac{d}{dr}(re^{-B(r)})\right\}-\frac{1}{2}(Rf_R-f)-e^{-B(r)}\left[\left\{\frac{2}{r}-B^{'}(r)\right\}f_R^{'}+f_R^{''}\right], \tag{32}$$

$$8\pi p_r=-\frac{f_R}{r^2}+\frac{1}{2}(Rf_R-f)+f_Re^{-B(r)}\left\{\frac{1}{r^2}+\frac{A'(r)}{r}\right\}+e^{-B(r)}\left\{\frac{2}{r}+A^{'}(r)\right\}f^{'}(R) \quad and \tag{33}$$

$$8\pi p_t=\frac{f_R}{r^2}\left[1+e^{-B(r)}\{rB'(r)-rA'(r)-1\}\right]-\frac{f}{2}+e^{-B(r)}\left[\left\{\frac{1}{r}+A'(r)-B'(r)\right\}f_R'+f_R''\right]. \tag{34}$$

Solving the above field Eqs. (32) to (34), one can obtain the expressions of energy density ρ, radial pressure p_r and transverse pressure p_t easily. We have also calculated these values for the concerned mass gap star and tabulated below. We have obtained that $p_t>p_r$ i.e. the existence of positive pressure anisotropy inside that massive compact object.

4 Physical analysis

Tables 1, 2, 3 and Figs. 1, 2, 3, 4.

• The recent observations of GWs from the binary merging events have given the NS study a new direction. At the same time, various observations of the existence of massive

Table 1 Model parameters of model-I for different values of ξ

Sl. no.	ξ	n	H	L	K	τ (km^{-2})
1	0.5	0.15	0.25	1.007	16.9856234125	0.0038562172
2	1.0	0.15	0.25	1.454	21.6235412873	0.0042654378
3	1.5	0.15	0.25	1.497	25.6481274392	0.0047368124
4	2.0	0.15	0.25	1.526	31.8647239852	0.0052134275
5	2.5	0.15	0.25	1.614	35.6542872398	0.0058374681

Table 2 Estimated values of p_r and p_t of the mass gap compact object from the model-I for different values of ξ

Sl. no.	ξ	p_r (dyne cm^{-2})	p_t (dyne cm^{-2})
1	0.5	4.4523235×10^{34}	5.563671×10^{35}
2	1.0	4.5458562×10^{34}	5.617843×10^{35}
3	1.5	4.6723713×10^{34}	5.694321×10^{35}
4	2.0	5.7229382×10^{35}	6.738662×10^{36}
5	2.5	5.8633761×10^{35}	6.848177×10^{36}

NSs through NICER surveys have motivated the researchers in this field and also made them more curious on these ultra-dense compact objects [96–98]. Due to their tremendous high density, these objects can reflect the GWs infalling on their surface which is nothing but the gravitational potential barrier. These compact objets can also develop some instabilities under rotation [99,100]. The GWs from a very distant merging event falls on the surface of these stars, it gets reflected at the photon sphere (after some time delay multiple reflection and refraction occurs). Most importantly, to generate GWEs it is essential that such massive compact objects should feature a photon sphere at $R_p = 3M_s$, M_s being the total mass of the compact star [101,102] and the minimum radius of such a star should be greater than the Buchdahl's radius $R_b = \frac{9}{4} M_s$ [103]. According to the studies the compact objects with radius in between $R_b \leq R_s \leq R_p$ are the most promising candidates to produce GWEs [104]. The characteristic echo times can be calculated as

$$T_{echo} \equiv \int_0^{M_{max}} e^{\frac{(A(r)-B(r))}{2}} dr. \tag{35}$$

Now, the characteristic echo frequencies can be obtained as

$$f_{GWEs} \simeq \frac{\pi}{T_{echo}}. \tag{36}$$

• The hydrostatic equilibrium condition for the stable compact stars can be obtained from the contracted Bianchi identities $\nabla^a T_{ab} = 0$, that gives the TOV equations as

$$\frac{dp_r}{dr} = \frac{2}{r}[p_t - p_r] - A^{'}(r)[p_r + \rho]. \tag{37}$$

The effective mass of the NS under this study in $f(R)$ modified gravity can be measured as

$$M(r) = 4\pi \int_0^r \rho r^2 dr. \tag{38}$$

We can obtain the total mass of the massive NS from the above Eq. (36). Further, $M(r) \to 0$ as $r \to 0$, shows that the mass function is regular at the center of the compact object (Fig. 5).

The smooth matching of the exterior and interior metric functions also confirmed the massive stable configuration of the mass gap compact object under investigation (Fig. 6).

• The study of TOV equation is also necessary for obtaining the stability of the model under various forces acting on the system as the hydrostatic force F_h, the gravitational force F_g, the anisotropic force F_a and the extra force due to the $f(R)$ modified gravity as $F_{f(R)}$. These forces can be represented as

$$F_h = -\frac{dp_r}{dr}, \tag{39}$$

$$F_g = -\frac{A^{'}(r)}{2}(\rho + p_r), \tag{40}$$

$$F_a = \frac{2}{r}(p_t - p_r) \quad and \tag{41}$$

$$F_{f(R)} = -\frac{\xi}{8\pi + 2\xi}(\rho^{'} + 2p_t^{'} + p_r^{'}). \tag{42}$$

Now, in terms of all the forces acting on the system, the TOV equation in $f(R)$ modified gravity can also be represented as

Table 3 Estimated values of p_c, ρ_s and ρ_c of the mass gap compact object from the model-I for different values of ξ

Sl. no.	ξ	p_c (dyne m^{-2})	ρ_s (g cm^{-3})	ρ_c (g cm^{-3})
1	0.5	5.6212345×10^{34}	$6.35525671 \times 10^{13}$	$7.558417423 \times 10^{14}$
2	1.0	5.7458522×10^{34}	$6.42261843 \times 10^{13}$	$7.625847371 \times 10^{14}$
3	1.5	5.8367513×10^{34}	$6.56537321 \times 10^{14}$	$7.736582928 \times 10^{15}$
4	2.0	5.8556482×10^{35}	$6.64825862 \times 10^{14}$	$7.785249541 \times 10^{15}$
5	2.5	6.1268618×10^{35}	$7.82572877 \times 10^{14}$	$8.915671378 \times 10^{15}$

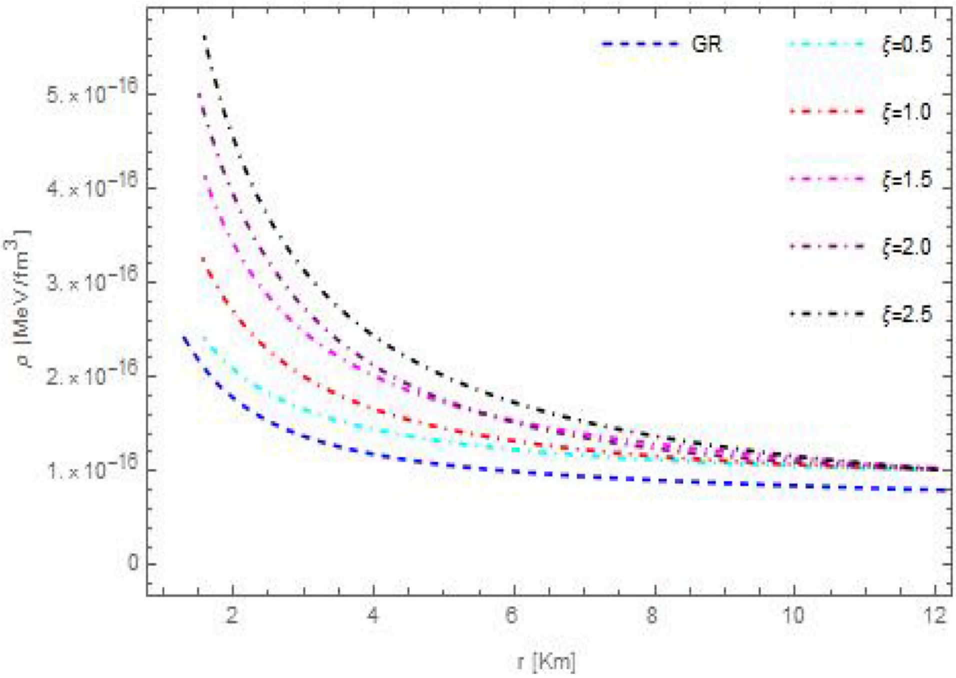

Fig. 1 Represents the variation of energy density ρ with radius r of the massive compact object (MG star in $GW230529$) for different values of ξ

$$F_h + F_g + F_a + F_{f(R)} = 0. \tag{43}$$

Interestingly, all these forces create the required hydrostatic equilibrium inside the star. This clearly revealed the spherically equilibrium structure of the massive anisotropic NSs under the investigation (Fig. 7).

• Various energy conditions like the null energy condition (NEC), the weak energy condition (WEC), the strong energy condition (SEC) and the dominant energy condition (DEC) are also obeyed if the subsequent inequalities are satisfied simultaneously at every point inside the stellar model. For this current model if all the following energy inequalities are satisfied in $f(R)$ gravity then the model will be physically realistic. All these conditions are given below

$$(\rho + p_t) \geq 0 \quad and \quad (\rho + p_r) \geq 0 : NEC \tag{44}$$

$$(\rho + p_t) > 0, \quad (\rho + p_r) > 0 \quad and \quad \rho \geq 0 : WEC \tag{45}$$

$$(\rho - p_r - 2p_t) \geq 0, \quad (\rho + p_r) \geq 0 \; and \; (\rho + p_t) \geq 0 : SEC \tag{46}$$

and

$$(\rho - p_r) \geq 0, \quad (\rho - p_t) \geq 0 \quad and \quad \rho \geq 0 : DEC \tag{47}$$

Significantly, all the necessary energy conditions are strongly satisfied in case of this current model. This clearly indicates the physical viability of the present model.

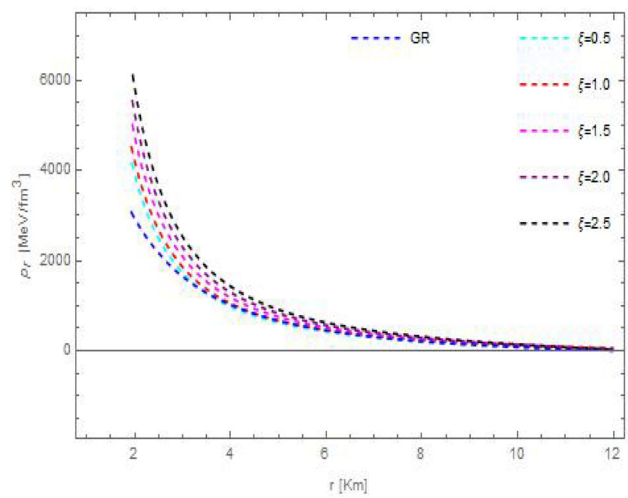

Fig. 2 Represent the variation of radial pressure p_r with radius r of the massive compact object (MG star in $GW230529$) for different values of ξ

• The compactness factor $u(r)$ of the compact star can be measured as

$$u(r) = \frac{1}{r} M(r). \tag{48}$$

The measured value of the compactness factor lies in between the proposed upper and lower bound of the compactness factor and also admits the Buchdahl limit. These values of $u(r)$ have confirmed the verification of all the inequalities in $f(R)$ gravity (Fig. 8).

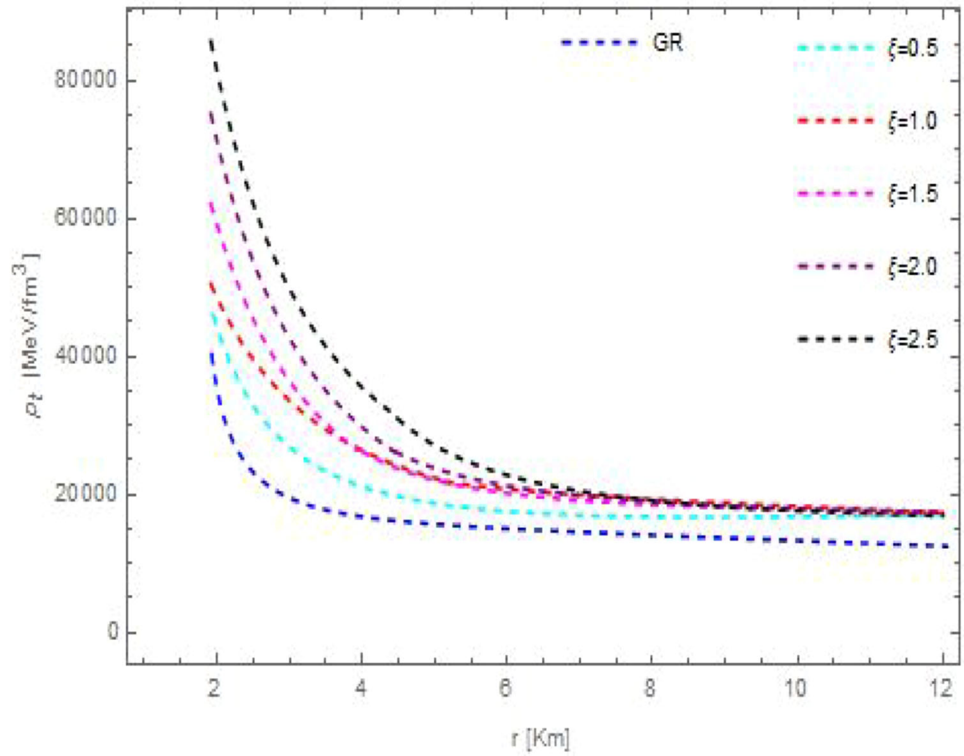

Fig. 3 Represent the variation of tangential pressure p_t with radius r of the massive compact object (MG star in $GW230529$) for different values of ξ

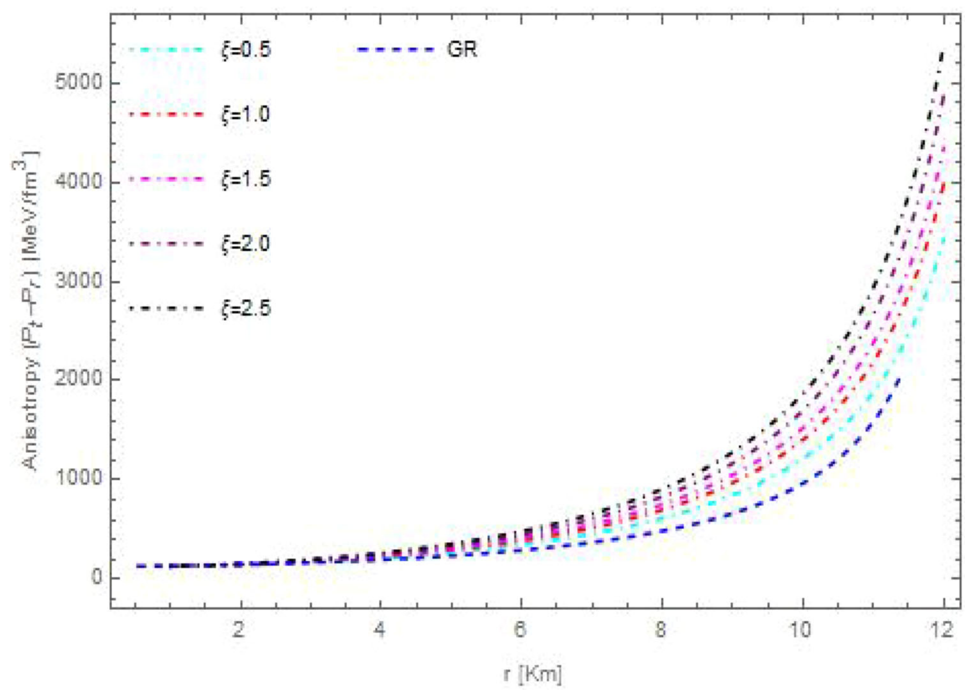

Fig. 4 Represents the variation of pressure anisotropy $p_t - p_r$ with radius r of the massive compact object (MG star in $GW230529$) for different values of ξ

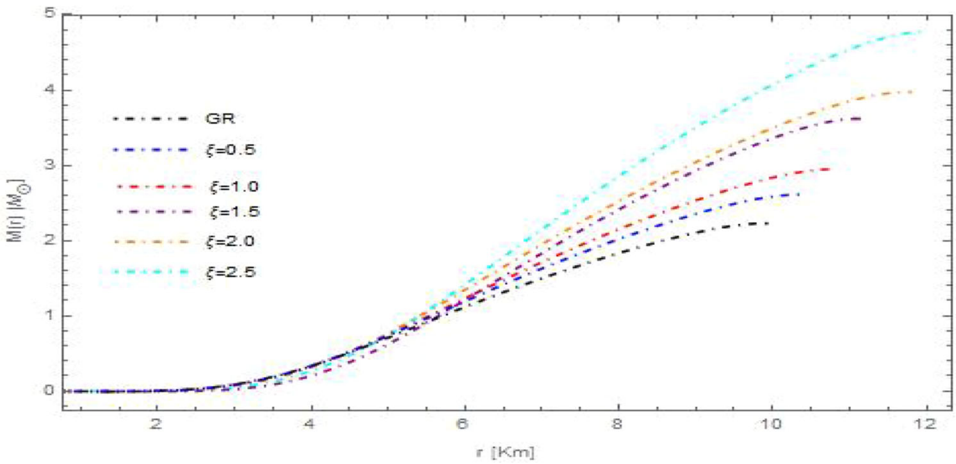

Fig. 5 Represents the variation of mass $M(r)[M_{\odot}]$ with radius r of the massive compact object for different values ξ

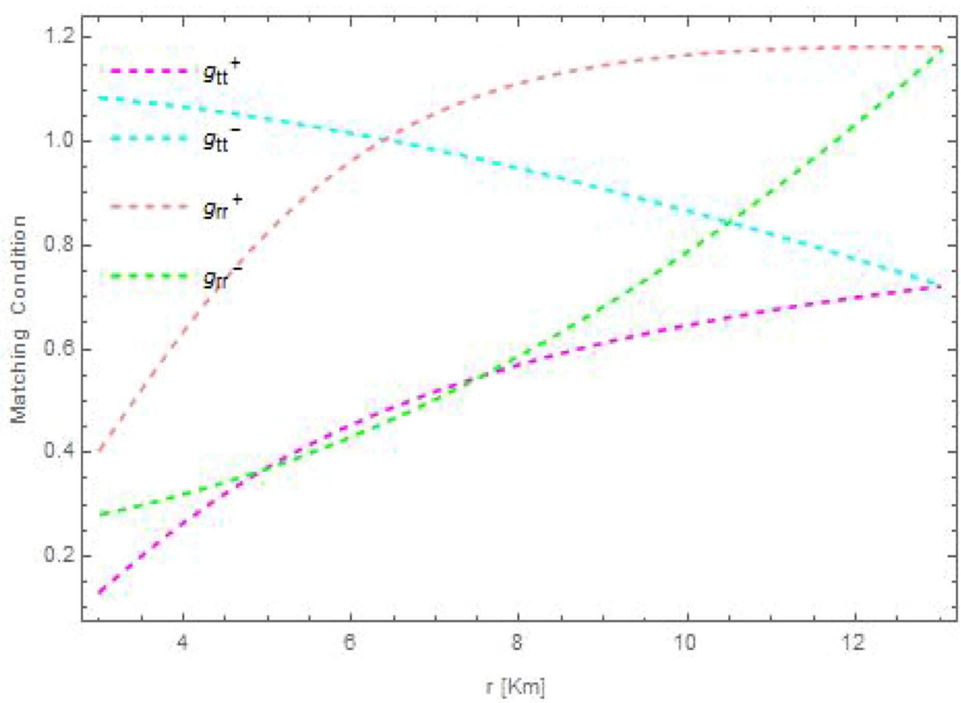

Fig. 6 Represents the matching conditions of the metric functions at the boundary of the massive compact star.

• The gravitational redshift function $Z_s(r)$ of the massive NS can be measured as

$$Z_s(r) = \frac{1}{\sqrt{\left(1 - \frac{2m(r)}{r}\right)}} - 1. \tag{49}$$

The value of the redshift is very significant to identify the compact object properly. The value $Z_s(r) > 0.5$ suggests that the compact object either is an exotic compact object or a black hole. To be a neutron star, the compact object must also satisfy $\frac{2M(r)}{R} < 1$. Further, the estimated redshift from the model lies in the range 0.4 *to* 0.5 which clearly reveals the mass gap compact object under the investigation is a supermassive NS. This also ensures the deep gravitational field and high redshift value also confirms the probability of generating the GWEs from the supermassive NS under the study (Fig. 9).

• The relativistic adiabatic index (Γ) also indicates the stability for the massive NSs. If $\Gamma > \frac{4}{3}$, the NS is under stability. The relativistic adiabatic index can be obtained as

$$\Gamma = \left(\frac{p_r + \rho}{p_r}\right) \frac{\partial p_r}{\partial \rho}. \tag{50}$$

The estimated values of Γ from the present model, for different values of ξ is tabulated below. The high value of Γ supports the massive compact structure of the star. Significantly,

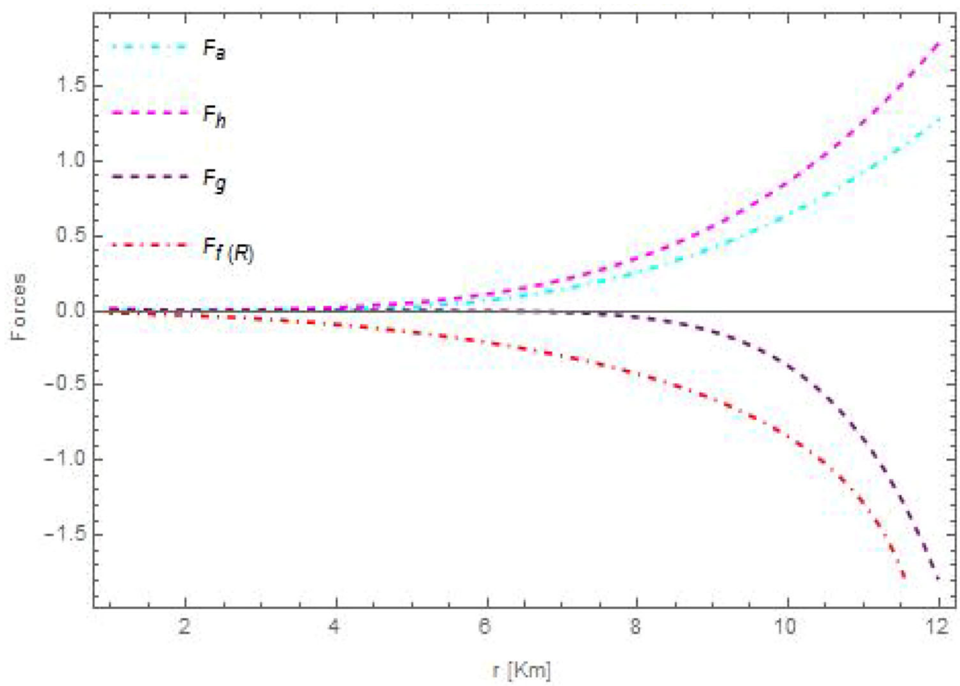

Fig. 7 Represents the variation of various forces with radius r for the modified TOV equation of the massive compact object

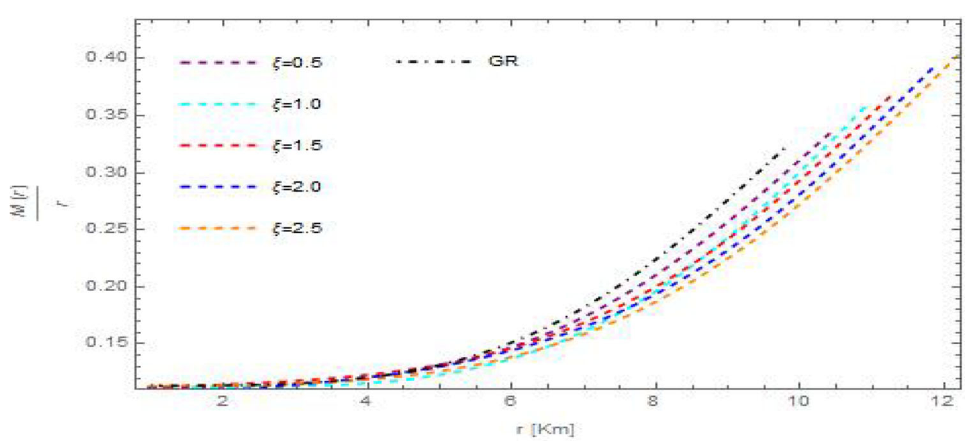

Fig. 8 Represents the variation of the compactness factor $u(r)$ with radius r of the massive compact object for different values of ξ

this value also indicates relatively soft EoS. Moreover, $\Gamma > \frac{4}{3}$ also ensures the stability of the compact object. This condition of Γ is mainly applicable in case of the NSs with isotropic configuration (Newtonian isotropic spheres) [106]. However, in case of the relativistic isotropic configuration of the compact objects (under Newtonian approximations), the threshold value of Γ differs which has been discussed elaborately in the reference [107]. Further, in order to realize the role of adiabatic index (Γ) on the stability of the massive relativistic and anisotropic compact objects, a more rigorous treatment is needed. In the context of relativistic approach for the anisotropic compact objects (under post-Newtonian approximation) the threshold value of Γ usually varies from $\frac{4}{3}$. The significant impact of the pressure anisotropy on the stability of the anisotropic compact objects in terms of Γ is discussed thoroughly in the references [108,109]. In Appendix-A, we have also discussed it in detail (Fig. 10).

• Again, to analysis the stability of the concerned mass gap compact object under the current investigation, sound velocities in two different directions have been considered as radial velocity of sound v_r^2 and transverse velocity of sound v_t^2. According to the causality conditions $0 \leq v_r^2 \leq 1$ and $0 \leq v_t^2 \leq 1$ should be obeyed strictly inside the stellar composition. The variations of the different sound velocities have been shown in the below figures. We have found that, for both models in $f(R)$ modified gravity, the sound velocities clearly satisfy the Herrera cracking conditions which implies $0 <| (v_t^2 - v_r^2) |< 1$ [47,54] (Tables 4, 5, 6, 7, 8, 9).

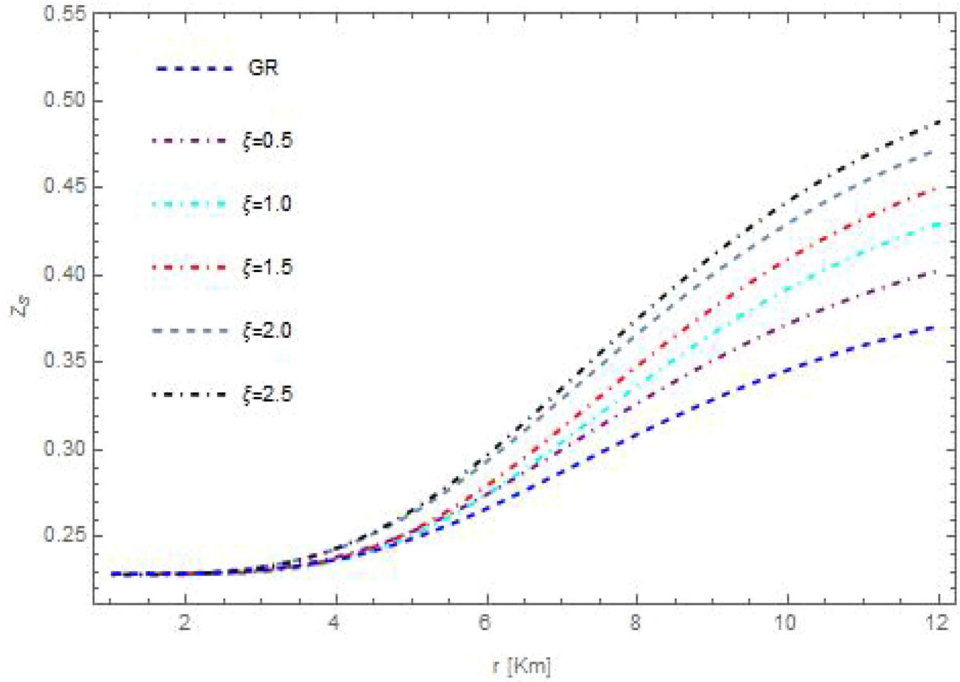

Fig. 9 Represents the variation of the gravitational redshift $Z_s(r)$ with radius r of the massive compact object for different values of ξ

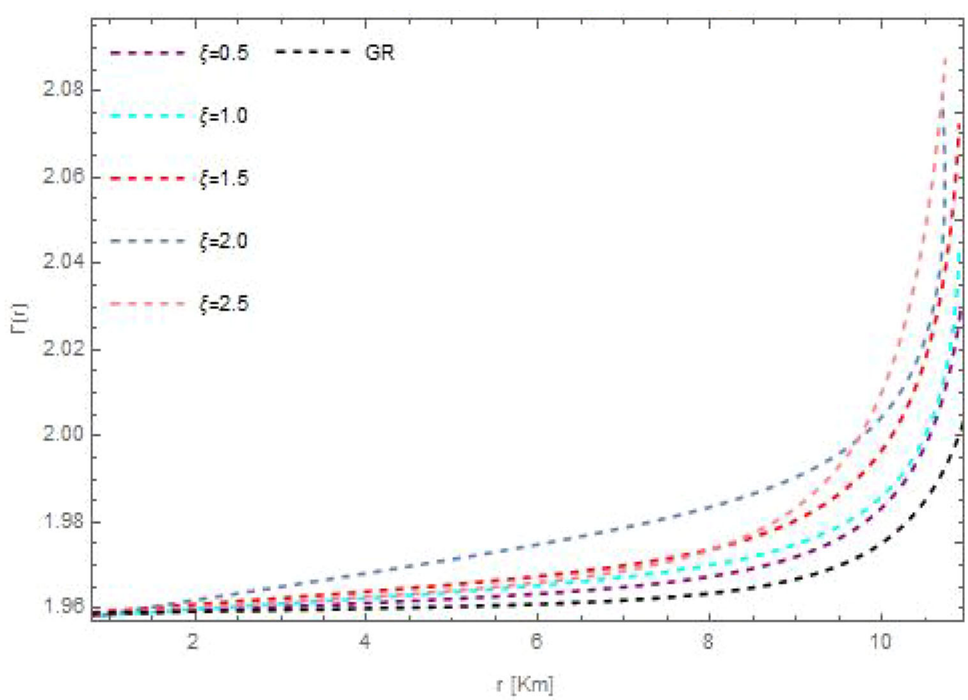

Fig. 10 Represents the variation of the adiabatic index Γ with radius r of the massive compact object for different values of ξ

5 Brief discussions and conclusion

In this particular work, some noteworthy results have been emerged during the investigation of mass gap compact objects in the framework of modified $f(R)$ gravity. Most importantly, two different realistic models (Model-I: $f(R) = R + \xi R^2$ and Model-II: $f(R) = Re^{\kappa R}$) of $f(R)$ gravity have been developed which have also been tested rigorously in the strong filed regime. Above all, this study have reshaped our conventional understanding of the NSs. In this exploration, the existence of the mass gap compact object has been established. At the same time, by investigating the properties, it has been revealed that the mass gap object is also a supermassive NS. This can be realized from the $mass-radius$ diagrams

Table 4 Estimated values of (Γ), ($\Delta^{'}$) and $Z_s(r)$ of the mass gap compact object form the model-I for different values of ξ

Sl. no.	ξ	Γ	$\Delta^{'}$	$Z_s(r)$
1	0.5	2.0225768435	0.0002958358	0.4075642547
2	1.0	2.0465425643	0.0003584214	0.4312732356
3	1.5	2.0650636492	0.0004833579	0.4564524529
4	2.0	2.0715637587	0.0005468235	0.4772646971
5	2.5	2.0826516586	0.0006764271	0.4985633574

Table 5 Estimated values of mass (M), radius (r), $u(r)$ and GWE of the mass gap compact object from the model-I for different values of ξ

Sl. no.	ξ	M ($M_{\odot}$)	r (km)	$u(r)$	GWE (f_{echo} in kHz)
1	0.5	2.6135874157	10.5827193425	0.3518274514	5.58412
2	1.0	2.9252584293	10.8974164784	0.3687534627	5.32681
3	1.5	3.6716371652	11.2756237751	0.3724983143	4.74379
4	2.0	4.1109753285	11.8736428752	0.3813583574	4.25674
5	2.5	4.8243945217	12.1651542827	0.3875098457	3.57865

Table 6 Model parameters of model-II for different values of ξ

Sl. no.	ξ	s_0	s_1	s_2
1	−0.01	0.35648	−0.85364	0.25207
2	−0.02	0.36972	−0.98523	0.32354
3	−0.03	0.37612	−1.00684	0.44973
4	−0.04	0.38724	−1.01536	0.52526
5	−0.05	0.39436	−1.02856	0.61423

Table 7 Estimated values of p_r and p_t of the mass gap compact object from the model-II for different values of ξ

Sl. no.	ξ	p_r (dyne cm^{-2})	p_t (dyne cm^{-2})
1	−0.01	5.4535735×10^{33}	4.561237×10^{34}
2	−0.02	5.5456261×10^{33}	4.623743×10^{34}
3	−0.03	6.6713842×10^{33}	5.695821×10^{34}
4	−0.04	6.7256282×10^{33}	6.738642×10^{34}
5	−0.05	7.8623761×10^{34}	7.948127×10^{35}

Table 8 Estimated values of p_c, ρ_s and ρ_c of the mass gap compact object from the model-II for different values of ξ

Sl. no.	ξ	p_c (dyne cm^{-2})	ρ_s (g cm^{-3})	ρ_c (g cm^{-3})
1	−0.01	4.6212345×10^{33}	$2.35525671 \times 10^{13}$	$3.558456223 \times 10^{14}$
2	−0.02	5.7458522×10^{33}	$2.42246843 \times 10^{13}$	$4.625254371 \times 10^{14}$
3	−0.03	5.8367513×10^{33}	$2.56917321 \times 10^{13}$	$4.736965292 \times 10^{14}$
4	−0.04	6.8539482×10^{33}	$3.64845862 \times 10^{13}$	$5.785749541 \times 10^{15}$
5	−0.05	7.1228618×10^{34}	$3.82722877 \times 10^{14}$	$5.915684278 \times 10^{15}$

obtained from the modified TOV equations according to the values of the model parameters. Moreover, the ramification of the modified $f(R)$ gravity has been explored and through which the structural evolution and stability under hydrostatic equilibrium of the supermassive NSs have been formalized. This investigation have also introduced the basic differences between GR and modified $f(R)$ gravity theories which have changed our ideas and conventional understandings on the NSs.

The present investigation delved into the study of the static interior of the supermassive NSs under spherical symmetry with anisotropic fluid distribution at the interior. The study of the signal $GW230529$ applying the Model-I gives the maximum mass and lowest possible radius of the mass gap (MG)

Table 9 Estimated values of mass (M), radius (r), $u(r)$ and GWE of the mass gap compact object from the model-II for different values of ξ

Sl. no.	ξ	M ($M_{\odot}$)	r (km)	$u(r)$	GWE (f_{echo} in kHz)
1	−0.01	2.5135874157	10.3827193429	0.3318274514	5.40235
2	−0.02	2.6525842935	10.7952384788	0.3387534627	5.23541
3	−0.03	2.6716371652	11.3632482757	0.3424983143	4.62183
4	−0.04	3.2109753285	11.5725467351	0.3513583574	4.14538
5	−0.05	3.6843945217	12.5623578623	0.3675098457	3.12692

object as (4.8 ± 0.15) $M_{\odot}$ and (12.16 ± 0.12) km respectively whereas from the Model-II through precise measurement we have obtained the mass and the corresponding radius as (3.7 ± 0.14) $M_{\odot}$ and (12.56 ± 0.17) km respectively. These estimated values from both the models in the background of modified $f(R)$ gravity, clearly revealed the existence of the supermassive NSs in the lower mass gap and also provides valuable constraints on the NS properties as well. Significantly, we have also studied the influence of ξ and have found out its physically valid range as well. Significantly, with the negative values of ξ, the upper limit of the compactness parameter increases slowly. This also is in a good agreement with the observations. Further, the extra force which arises due to anisotropy, opposes the strong gravitational force with increasing mass of the NSs clearly supports the MG stars and allows the stars to contain more mass with higher compactness.

We are also very concerned on investigating the stability of these MG stars in the context of modified $f(R)$ gravity. We have examined the stability of these NSs applying different stability criterion including the Zeldovich condition, energy conditions and the speed of sound. Our investigation has clearly revealed that all the required conditions have been satisfied successfully in the framework of $f(R)$ gravity within the specific range of the parameters. This is also confirmed the physical validity of the current models. The feasible range of ξ, we have obtained as $0.5 \leq \xi \leq 2.5$ and $-0.01 \leq \xi \leq -0.05$ from the Model-I and Model-II respectively. So, it is clear that in case of Model-II, we can achieve the maximum possible mass of the supermassive NSs in the lower mass gap with small negative values of ξ compared to the positive values of ξ as in Model-I. The stability of the MG compact objects with the maximum mass can also be validated through precise measurement of the various properties like core energy density, radial pressure and transverse pressure etc. The core density of the MG objects is about 2.5 times the nuclear density and the surface density is about 1.6 times the nuclear density. This provides a better fit with most of the observed NSs (pulsars). In case of $f(R)$ gravity, the essential conditions for a physically consistent and realistic models must obey the conditions like $\frac{d\rho}{dr} < 0$, $\frac{dp_r}{dr} < 0$ and $\frac{dp_t}{dr} < 0$. These conditions clearly indicates that the central density, radial pressure and transverse pressure decreases outward from the centre of the MG object. Further, these conditions also reveal the stability under hydrostatic equilibrium and realistic configuration of the massive compact objects in the lower mass gap.

Significantly, all the energy conditions are also satisfied by both models with the presence of anisotropic fluid distribution inside massive NSs. These conditions strongly ensures the existence of physically meaningful and stable compact object indeed. Moreover, the values of the gravitational redshift for the NSs under the influence of strong gravitational filed clearly depicts the evolution of such mass gap compact objects. the stability of such objects are also satisfied by the estimated values of the adiabatic index. Further, the cracking conditions and the causality conditions are also strongly satisfied for the mass gap compact objects.

We have also got the clear evidence about the formation of GWEs from those mass gap NSs due to their supermassive structure and high compactness. Significantly, this reflects their ultra-compact structure and we can understand their structural evolution with super dense core matter as well. These mass gap stars should have a photon sphere outside their structure. The formation of GWEs can be the testing tool for various compact star models in modified gravity theories also. The GWEs produces from the infalling GWs in the potential barrier of these stars also helps to remove their non-linear instabilities due to their high compactness. The estimated frequencies of the GWEs play a very significant role to understand the properties of these stars deeply. This also give us information about their internal composition and physical properties.

Conclusively, this current work has given a singularity free model of a supermassive anisotropic NS in the framework of $f(R)$ modified gravity. The mass of the investigated NS lies in the mass gap domain. The pressure anisotropy has a crucial role on the structural evolution of the massive NSs. The outcome of this work have been analyzed rigorously. Significantly, all the outcomes are highly compatible with various other astrophysical observations. Further, all assumptions and considerations during the work are properly validated through their physical significance. The comparison of results with GR has made this work very crucial and significant. Moreover, by considering $\xi \to 0$, we can also recover the GR results in four dimensions as well. Finally, the present work significantly helps to provide better understanding on the supermassive NSs in the lower mass gap in the context of recent astrophysical observations.

Acknowledgements MB wishes to thank IUCAA, PUNE for visiting associateship.

Data Availability Statement This manuscript has no associated data. [Authors' comment: This article has no associated data as the work is completely theoretical in nature.]

Code Availability Statement This manuscript has no associated code/software. [Authors' comment: Code/Software sharing not applicable to this article as no code/software was generated or analysed during the current study.]

Declarations

Conflict of interest Author declares that he does not have any financial, commercial, legal relationship with organizations or with the people working with him that could influence the research.

Funded by SCOAP^3.

Appendix-A

In the relativistic treatment, the dynamical stability of the massive compact objects under radial perturbations (for anisotropic matter distributions) has shown that pressure anisotropy modifies the instability range of (Γ) in a non-trivial way [109]. Within the Newtonian limit the unstable range of adiabatic index (Γ) can be expressed as

$$\Gamma < \frac{4}{3} - \left[\frac{4(p_{r0} - p_{t0})}{3|p_{r0}|r}\right]_{max}, \tag{51}$$

where the subscript 0 represents the quantity under equilibrium. The above Eq. (51) clearly indicates that the instability range of Γ depends on the anisotropic factor $(p_{r0} - p_{t0})$ (sign of the anisotropic factor). So, it is very clear that in case of the compact stars with anisotropic matter distribution, pressure anisotropy may decrease or increase and play a very important role on the stability of the compact object.

Furthermore, under the post-Newtonian approximation, the corresponding expression of Γ acquires an additional gravitational contribution and the instability range of (Γ) becomes

$$\Gamma < \frac{4}{3} - \left[\frac{4(p_{r0} - p_{t0})}{3|p_{r0}|r} - \frac{8\pi r p_{r0}}{3|p_{r0}|}\right]_{max}. \tag{52}$$

The above Eq. (52) clearly depicts that the relativistic effects (gravitational terms) generally increase the unstable range of the adiabatic index (Γ) due to the regenerative action of p_r.

Therefore, the simple bound $(\Gamma > \frac{4}{3})$ cannot be invoked as a general stability criterion for anisotropic relativistic stars. A rigorous assessment would require evaluating the model's adiabatic index throughout the configuration and verifying that it remains outside the instability window defined by the above expressions. While a detailed perturbative analysis lies beyond the scope of the present work, these considerations should be kept in mind when interpreting the role of (Γ) in the stability of anisotropic compact objects.

References

1. C.M. Will, The confrontation between general relativity and experiment. Living Rev. Relativ. **17**, 4 (2014)
2. B.P. Abbott et al., Tests of general relativity with $GW170817$. Phys. Rev. Lett. **123**, 011102 (2019)
3. J. Harada, Connection independent formulation of general relativity. Phys. Rev. D **101**, 024053 (2020)
4. K. Akiyama et al., First $M87$ Event Horizon Telescope results. I. The shadow of the supermassive black hole. Astrophys. J. Lett. **875**(1), L1 (2019)
5. K. Akiyama et al., First Sagittarius A* Event Horizon Telescope results. I. The shadow of the supermassive black hole in the center of the Milky Way. Astrophys. J. Lett. **930**(2), L12 (2022)
6. A.G. Riess et al., Observational evidence from supernovae for an accelerating Universe and a cosmological constant. Astron. J. **116**, 1009 (1998)
7. S. Perlmutter et al., Measurements of omega and lambda from 42 high-redshift supernovae. Astron. J. **517**, 565 (1999)
8. D.N. Spergel et al., First year Wilkinson Microwave Anisotropy Probe (WMAP) observations: determination of cosmological parameters. Astrophys. J. Suppl. **148**, 175–194 (2003)
9. S.M. Carroll, V. Duvvuri, M. Trodden, M.S. Turner, Is cosmic speed-up due to new gravitational physics? Phys. Rev. D **70**, 043528 (2004)
10. D.J. Einstein et al., Detection of the baryon acoustic peak in the large-scale correlation function of SDSS luminous red galaxies. Astrophys. J. **633**, 560–574 (2005)
11. G.J. Olmo, D.R. Garcia, A. Wojnar, Stellar structure models in modified theories of gravity: lessons and challenges. Phys. Rep. **876**, 1 (2020)
12. T. Harko, F.S.N. Lobo, S. Nojiri, S.D. Odintsov, $f(R, T)$ gravity. Phys. Rev. D **84**(2), 024020 (2011)
13. M. Bandyopadhyay, R. Biswas, Investigating the equation-of-state, stability and mass-radius relationship of anisotropic and massive neutron stars embedded in $f(R, T)$ modified gravity. Int. J. Geom. Methods Mod. Phys. **21**(12), 2450203 (2024)
14. M. Bandyopadhyay, R. Biswas, Isolated compact star RXJ1856.5 - 3754 in $f(R, T)$ modified gravity in Tolman–Kuchowicz spacetime. Phys. Lett. A **518**, 129676 (2024)

15. M. Bandyopadhyay, R. Biswas, Cosmology in $f(R, T)$ modified gravity: unified dark matter and dark energy model constrained by current observations. Phys. Scr. **99**, 115008 (2024)
16. P.H.R.S. Moraes, P.K. Sahoo, The simplest non-minimal matter geometry coupling in the $f(R, T)$ cosmology. Eur. Phys. J. C **77**(7), 1–8 (2017)
17. R. Lobato et al., Neutron stars in $f(R, T)$ gravity using realistic equations of state in the light of massive pulsars and $GW170817$. J. Cosmol. Astropart. Phys. **12**, 039 (2020)
18. M. Bandyopadhyay, R. Biswas, Repulsive gravitational force and quintessence field in $f(T)$ gravity: How anisotropic compact stars in strong energy condition behave. Mod. Phys. Lett. A **36**(07), 2150044 (2021)
19. M. Bandyopadhyay, R. Biswas, Nuclear matter equation of state and stability of charged compact stars embedded in $f(T)$ modified gravity, under cosmic acceleration. Int. J. Geom. Methods Mod. Phys. **21**(05), 2450097 (2024)
20. S.H. Hendi, G.H. Bordbar, B.E. Panah, S. Panahiyan, Modified TOV in gravity's Rainbow: properties of neutron stars and dynamical stability conditions. J. Cosmol. Astropart. Phys. **2016**(09), 013 (2016)
21. M. Bandyopadhyay, R. Biswas, Impacts of modified Chaplygin gas on super-massive neutron stars embedded in quintessence field with $f(T)$ gravity. Int. J. Mod. Phys. D **32**(03), 2350006 (2023)
22. A.V. Astashenok, S.D. Odintsov, A. De la Cruz-Dombriz, The realistic models of relativistic stars in $f(R) = R + \alpha R^2$ gravity. Class. Quantum Gravity **34**(20), 205008 (2017)
23. M. Bandyopadhyay, Structural features and physical properties of charged X-ray binaries in $f(T)$ modified gravity under Tolman–Kuchowicz spacetime. Euro. Phys. J. Plus **140**(1), 1–29 (2025)
24. T.P. Sotiriou, V. Faraoni, $f(R)$ theories of gravity. Rev. Mod. Phys. **82**, 451 (2010)
25. G.G.L. Nashed, S. Capozziello, Anisotropic compact stars in $f(R)$ gravity. Euro. Phys. J. C **81**(5), 1–20 (2021)
26. T. Kobayashi, K.I. Maeda, Can higher curvature corrections cure the singularity problem in $f(R)$ gravity? Phys. Rev. D **79**(2), 024009 (2009)
27. A.M. Nzioki, S. Carloni, R. Goswami, P.K. Dunsby, New framework for studying spherically symmetric static solutions in $f(R)$ gravity. Phys. Rev. D **81**(8), 084028 (2010)
28. H. Rizwanakausar, I. Noureen, M.U. Shahzad, Dynamical analysis of charged anisotropic spherical star in $f(R)$ gravity. Eur. Phys. J. Plus **130**(10), 204 (2015)
29. S.I. Nojiri, S.D. Odintsov, Introduction to modified gravity and gravitational alternative for dark energy. Int. J. Geom. Methods Mod. Phys. **4**(01), 115–145 (2007)
30. S. Capozziello, M. De Laurentis, Extended theories of gravity. Phys. Rep. **509**(4–5), 167–321 (2011)
31. T. Clifton, P.G. Ferreira, A. Padilla, C. Skordis, Modified gravity and cosmology. Phys. Rep. **513**(1–3), 1–189 (2012)
32. K. Bamba, S.I. Nojiri, S.D. Odintsov, Modified gravity: walk through accelerating cosmology. arXiv preprint arXiv:1302.4831 (2013)
33. D. Paul, S. Kalita, MOND equivalence of $f(R)$ gravity theory in solar system and cosmological scalarons. arXiv preprint arXiv:2406.00351 (2024)
34. M. Bandyopadhyay, Exploring the impact of dark energy on the equation of state, physical properties and stability of charged anisotropic neutron stars in higher dimension. Int. J. Geom. Methods Mod. Phys. https://doi.org/10.1142/S0219887825502470
35. M. Bandyopadhyay, Evolution of black holes and anisotropic neutron stars under late time cosmic acceleration. Ph.D. Thesis, Jadavpur University, Kolkata, West Bengal (2024). http://hdl.handle.net/10603/605889
36. M. Bandyopadhyay, Evolution of anisotropic and charged neutron stars in the lower mass gap with a perturbative approach in f(T,) gravity: constraining the equation of state and physical properties in the light of NICER observations. Mod. Phys. Lett. A (2025). https://doi.org/10.1142/S0217732325501718
37. A. de la Cruz-Dombriz, D. Saez-Gomez, Black holes, cosmological solutions, future singularities, and their thermodynamical properties in modified gravity theories. Entropy **14**(9), 1717–1770 (2012)
38. M. Bandyopadhyay, R. Biswas, Investigation on the stability and quantum phase transition of the charged rotating Kiselev black hole embedded in Quintessence field with quantum fluctuation of entropy. Int. J. Geometr. Methods Mod. Phys. **21**(01), 2450021 (2024). https://doi.org/10.1142/S021988782450021X
39. M. Bandyopadhyay, R. Biswas, Generalized model of interacting dark energy and dark matter: phase portrait analysis for evolving universe. Mod. Phys. Lett. A **36**(40), 2150275 (2021). https://doi.org/10.1142/S0217732321502758
40. M. Bandyopadhyay, R. Biswas, Cosmology in $f(R, T)$ modified gravity: unified dark matter and dark energy model constrained by current observations. Phys. Scr. **99**, 115008 (2024). https://doi.org/10.1088/1402-4896/ad80e9
41. S.M. Hossein, F. Rahaman, J. Naskar, M. Kalam, S. Ray, Anisotropic compact stars with variable cosmological constant. Int. J. Mod. Phys. D **21**(13), 1250088 (2012)
42. L. Herrera, N.O. Santos, Local anisotropy in self-gravitating systems. Phys. Rep. **286**(2), 53–130 (1997)
43. G. Abbas, M. Zubair, G. Mustafa, Anisotropic strange quintessence stars in $f(R)$ gravity. Astrophys. Space Sci. **358**(2), 26 (2015)
44. B.V. Ivanov, Analytical study of anisotropic compact star models. Eur. Phys. J. C **77**, 1–12 (2017)
45. D. Deb, S.R. Chowdhury, S. Ray, F. Rahaman, B.K. Guha, Relativistic model for anisotropic strange stars. Ann. Phys. **387**, 239–252 (2017)
46. G. Abbas, H. Nazar, Complexity factor for anisotropic source in non-minimal coupling metric $f(R)$ gravity. Eur. Phys. J. C **78**, 1–12 (2018)
47. L. Herrera, W. Barreto, General relativistic polytropes for anisotropic matter: the general formalism and applications. Phys. Rev. D **88**(8), 084022 (2013)
48. M. Azam, S.A. Mardan, I. Noureen, M.A. Rehman, Charged cylindrical polytropes with generalized polytropic equation of state. Eur. Phys. J. C **76**, 1–9 (2016)
49. S. Khan, S.A. Mardan, M.A. Rehman, Framework for generalized polytropes with complexity factor. Eur. Phys. J. C **79**(12), 1037 (2019)
50. S.A. Mardan, M. Rehman, I. Noureen, R.N. Jamil, Impact of generalized polytropic equation of state on charged anisotropic polytropes. Eur. Phys. J. C **80**(2), 119 (2020)
51. S. Khan, S.A. Mardan, M.A. Rehman, Study of charged generalized polytropes with complexity factor. Eur. Phys. J. Plus **136**(4), 404 (2021)
52. H. Komatsu, Y. Eriguchi, I. Hachisu, Rapidly rotating general relativistic stars-I. Numerical method and its application to uniformly rotating polytropes. Mon. Not. R. Astron. Soc. **237**(2), 355–379 (1989)
53. L. Herrera, W. Barreto, Newtonian polytropes for anisotropic matter: general framework and applications. Phys. Rev. D **87**(8), 087303 (2013)
54. L. Herrera, A. Di Prisco, W. Barreto, J. Ospino, Conformally flat polytropes for anisotropic matter. Gen. Relativ. Gravit. **46**, 1827 (2014)
55. R.C. Freitas, S.V.B. Goncalves, Polytropic equation of state and primordial quantum fluctuations. Eur. Phys. J. C **74**, 1–11 (2014)
56. S.A. Mardan, A.A. Siddiqui, I. Noureen, R.N. Jamil, New models of charged anisotropic polytropes with radiation density. Eur. Phys. J. Plus **135**(1), 1–18 (2020)

57. K. Henttunen, T. Multamaki, I. Vilja, Stellar configurations in $f(R)$ theories of gravity. Phys. Rev. D **77**(2), 024040 (2008)
58. N. Deruelle, M. Sasaki, Y. Sendouda, Junction conditions in $f(R)$ theories of gravity. Prog. Theor. Phys. **119**(2), 237–251 (2008)
59. M.S.R. Delgaty, K. Lake, Physical acceptability of isolated, static, spherically symmetric, perfect fluid solutions of Einstein's equations. Comput. Phys. Commun. **115**(2–3), 395–415 (1998)
60. P. Tamta, P. Fuloria, Study of anisotropic stellar objects, a revisit to Buchdahl metric potential. Int. J. Mod. Phys. D **31**(08), 2250057 (2022)
61. J.M. Senovilla, Junction conditions for $f(R)$ gravity and their consequences. Phys. Rev. D **88**(6), 064015 (2013)
62. S. Chandrasekhar, Astrophys. J. **74**, 81 (1931)
63. F. Mullally, C. Badenes, S.E. Thompson, R. Lupton, Astrophys. J. **707**, L51 (2009)
64. P.B. Demorest, T. Pennucci, S.M. Ransom, M.S.E. Roberts, J.W.T. Hessels, Nature **467**, 1081 (2010)
65. M.L. Rawls et al., Astrophys. J. **730**, 25 (2011)
66. N.-B. Zhang, B.-A. Li, Astrophys. J. **879**, 99 (2019)
67. R. Abbott et al., $GW190814$: gravitational waves from the coalescence of a 23 $M_{\odot}$ black hole with a 2.6 $M_{\odot}$ compact object. Astrophys. J. Lett. **896**, L44 (2020)
68. L. Mazwi, S. Razzaque, L. Nayadzani, On non-detection of gamma-ray bursts in three compact binary merger events detected by LIGO. Mon. Not. R. Astron. Soc. **531**(1), 2162–2167 (2024)
69. Z.-W. Du et al., How to identify the object with a mass range of $(2.2--3\ M_{\odot})$ in the merger of compact star systems. Astrophys. J. **985**(1), 42 (2025)
70. A.G. Abac et al., Observation of gravitational waves from the coalescence of a $2.5-4.5\ M_{\odot}$ compact object and a neutron star. Astrophys. J. Lett. **970**, L34 (2024)
71. J. Antoniadis et al., A massive pulsar in a compact relativistic binary. Science **340**(6131), 1233232 (2013)
72. J. Poutanen et al., The effect of accretion on the measurement of neutron star mass and radius in the low-mass X-ray binary $4U1608-52$. Mon. Not. R. Astron. Soc. **442**(4), 3777–3790 (2014)
73. R. Goswami, A.M. Nzioki, S.D. Maharaj, S.G. Ghosh, Collapsing spherical stars in $f(R)$ gravity. Phys. Rev. D **90**(8), 084011 (2014)
74. P. McDonald et al., SDSS. Astrophys. J. Suppl. **163**, 80 (2006)
75. D.N. Spergel et al., WMAP Collaboration. Astrophys. J. Suppl. **148**, 175 (2003)
76. T. Clifton, P. Dunsby, R. Goswami, A.M. Nzioki, On the absence of the usual weak-field limit, and the impossibility of embedding some known solutions for isolated masses in cosmologies with $f(R)$ dark energy. Phys. Rev. D **87**(6), 063517 (2013)
77. C. Schimdt et al., Astron. Astrophys. **463**, 405 (2007)
78. S. Capozziello, V. Faraoni, Beyond Einstein gravity: a survey of gravitational theories for cosmology and astrophysics. in *Fundamental Theories of Physics*, vol. 170 (Springer, 2010). (**ISBN978-94-007-0164-9**)
79. A. de la Cruz-Dombriz, D. Saez-Gomez, Entropy **14**, 1717 (2012)
80. S. Nojiri, S.D. Odintsov, Phys. Rep. **505**, 59 (2011)
81. V. Cardoso, E. Franzin, P. Pani, Is the gravitational-wave ringdown a probe of the event horizon? Phys. Rev. Lett. **116**, 171101 (2016)
82. V. Cardoso, P. Pani, Testing the nature of dark compact objects: a status report. Living Rev. Relativ. **22**, 4 (2019)
83. C. Vlachos, E. Papantonopoulos, K. Destounis, Echoes of compact objects in scalar–tensor theories of gravity. Phys. Rev. D **103**, 044042 (2021)
84. N. Chatzifotis, C. Vlachos, K. Destounis, E. Papantonopoulos, Stability of black holes with non-minimally coupled scalar hair to the Einstein tensor. Gen. Relativ. Gravit. **54**, 49 (2022)
85. P. Pani, V. Ferrari, On gravitational-wave echoes from neutron-star binary coalescences. Class. Quantum Gravity **35**, 15LT01 (2018)
86. M. Mannarelli, F. Tonelli, Gravitational wave echoes from strange stars. Phys. Rev. D **97**, 123010 (2018)
87. A. Urbano, H. Veermäe, On gravitational echoes from ultracompact exotic stars. J. Cosmol. Astropart. Phys. **04**, 011 (2019)
88. J. Bora, U.D. Goswami, Radial oscillations and gravitational wave echoes of strange stars for various equations of state. Mon. Not. R. Astron. Soc. **502**, 1557 (2021)
89. C. Zhang, Gravitational wave echoes from interacting quark stars. Phys. Rev. D **104**, 083032 (2021)
90. J. Bora, U.D. Goswami, Radial oscillations and gravitational wave echoes of strange stars with nonvanishing lambda. Astropart. Phys. **143**, 102744 (2022)
91. J. Bora, D.J. Gogoi, U.D. Goswami, Strange stars in $f(R)$ gravity Palatini formalism and gravitational wave echoes from them. J. Cosmol. Astropart. Phys. **09**, 057 (2022)
92. P. Tamta, P. Fuloria, Study of anisotropic stellar objects, a revisit to Buchdahl metric potential. Int. J. Mod. Phys. D **31**(08), 2250057 (2022)
93. A.A. Starobinsky, A new type of isotropic cosmological models without singularity. Phys. Lett. B **91**(1), 99–102 (1980)
94. N.D. Birrell, P.C.W. Davies, *Quantum Fields in Curved Space* (Cambridge University Press, Cambridge, 1984)
95. J.M. Senovilla, Junction conditions for $f(R)$ gravity and their consequences. Phys. Rev. D **88**(6), 064015 (2013)
96. M. Miller et al., $PSRJ0030+0451$ mass and radius from NICER data and implications for the properties of neutron star matte. Astrophys. J. Lett. **887**, L24 (2019)
97. T. Riley et al., A NICER view of the massive pulsar $PSRJ0740+6620$ informed by radio timing and XMM-Newton Spectroscopy. Astrophys. J. Lett. **918**(2), L27 (2021)
98. N.K. Patra, A. Venneti, Sk Md A. Imam, A. Mukherjee, B.K. Agrawal, Systematic analysis of the impacts of symmetry energy parameters on neutron star properties. *Phys. Rev. C***107**, 055804 (2023)
99. N. Comins, B.F. Schutz, S. Chandrasekhar, On the Ergoregion instability. Proc. R. Soc. Lond. A. Math. Phys. Sci. **364**, 211 (1978)
100. C.B.M.H. Chirenti, L. Rezzolla, On the Ergoregion instability in rotating gravastars. Phys. Rev. D **78**, 084011 (2008)
101. V. Cardoso et al., Light rings as observational evidence for event horizons: long-lived modes, ergoregions and nonlinear instabilities of ultracompact objects. Phys. Rev. D **90**, 044069 (2014)
102. J. Keir, Slowly decaying waves on spherically symmetric spacetimes and an instability of ultracompact neutron stars. arXiv:1404.7036
103. H.A. Buchdahl, General relativistic fluid spheres. Phys. Rev. **116**, 1027 (1959)
104. P. Burikham, T. Harko, M.J. Lake, Mass bounds for compact spherically symmetric objects in generalized gravity theories. Phys. Rev. D **94**, 064070 (2016)
105. L. Herrera, Stability of the isotropic pressure condition. Phys. Rev. D **101**, 104024 (2020)
106. S. Chandrasekhar, The dynamical instability of gaseous masses approaching the Schwarzschild limit in general relativity. Astrophys. J. **140**, 417–433 (1964)
107. H. Bondi, The contraction of gravitating spheres. Proc. R. Soc. Lond. A **281**, 39–48 (1964)
108. R. Chan et al., Dynamical instability for radiating anisotropic collapse. Mon. Not. Roy. Astron. Soc. **265**(3), 533–544 (1993)
109. R. Chan et al., Dynamical instability in the collapse of anisotropic matter. Class. Quantum Gravity **9**, L133 (1992)